(20) I. Antonini, F. Claudi, G. Cristalli, P. Franchetti, M. Grifantini, and S. Martelli, *J. Med. Chem.*, **25**, 1258 (1982).

ACKNOWLEDGMENTS

This paper, number 3 in a series on platelet aggregation inhibitors, was presented in part at the VII International Symposium on Medicinal Chemistry in Torremolinos (Malaga), Spain, September 1980 (Abstract P40).

The authors thank A. Biondi for elemental analysis, F. Lupidi for NMR spectra, and I. Pennacchioli for typing the manuscript.

Degradation and Epimerization Kinetics of Moxalactam in Aqueous Solution

NAOFUMI HASHIMOTO ˣ, TAKENOBU TASAKI, and HIROYOSHI TANAKA

Received September 7, 1982, from the *Shionogi Research Laboratories, Shionogi & Co., Ltd., Fukushima-ku, Osaka 553, Japan.* Accepted for publication January 26, 1983.

Abstract □ The kinetics of epimerization and degradation of moxalactam in aqueous solution was investigated by HPLC. The pH–rate profiles of the degradation and epimerization were determined separately over the pH range of 1.0–11.5 at 37°C and constant ionic strength 0.5. The degradation and simultaneous epimerization were followed by measuring both of the residual *R*- and *S*-epimers of moxalactam and were found to follow pseudo-first-order kinetics. The degradation was subjected to hydrogen ion and hydroxide ion catalyses and influenced by the dissociation of the side chain phenolic group. The epimerization rates were influenced significantly in the acidic region by the dissociation of the side chain carboxylic acid group and in the basic region by hydroxide ion catalysis. The pH–degradation rate profile of moxalactam showed a minimum degradation rate constant between pH 4.0 and 6.0. The pH–epimerization rate profiles of moxalactam showed minimum epimerization rate constants at pH 7.0. The epimerization rate constants of the *R*- and *S*-epimers were not very different.

Keyphrases □ Moxalactam—degradation and epimerization in aqueous solutions, kinetics, HPLC □ Degradation—moxalactam in aqueous solutions, kinetics, epimerization □ Epimerization—moxalactam in aqueous solutions, kinetics, degradation □ Kinetics—moxalactam degradation and epimerization in aqueous solutions, HPLC

Stereoisomers, occurring widely in nature, display different biological and pharmacological effects than their racemic mixtures. Many β-lactam antibiotics have stereoisomers with different antibacterial activities (1). Few reports (2, 3) describe the kinetics of the epimerization of β-lactam antibiotics, a process which should offer valuable information for predicting and improving antibacterial activity.

Moxalactam (6059-S)[1] is a new semisynthetic (4), broad-spectrum (5) 1-oxacephalosporin which exists as the *R*- and *S*-epimers, epimeric at C-7. The *in vitro* activity of the *R*-epimer is twice that of the *S*-epimer (1). In the present study, the epimerization and degradation of moxalactam were investigated kinetically.

EXPERIMENTAL

Materials—*R*- and *S*-epimers of moxalactam disodium and decarboxy-moxalactam monosodium (decarboxylated in the 7-side chain)[1] were used as obtained. All other chemicals were of reagent grade. Water was purified with an ion-exchange column and distilled before being used.

pH—The pH of the solution was controlled throughout the reaction by a pH-stat[2]. The titrated volume of diluted hydrochloric acid or sodium hydroxide solution was at most 2% of the reaction volume. The ionic strength was adjusted to 0.5 by the addition of potassium chloride. No significant pH change was observed throughout the reaction. The pH meter[3] was standardized with the combination of standard buffer solutions of pH 4 and 7 or pH 7 and 9 at the temperature of the kinetic experiments.

Analytical Procedures—HPLC[4] was used to determine the concentrations of *R*- and *S*-epimers of moxalactam and decarboxy-moxalactam. Quantification was based on integration of peak areas using an integrator[5]. The elution was carried out on a 4.0 × 250-mm stainless steel column packed with octadecylsilane chemically bonded on silica gel[6] at room temperature. The mobile phase employed to resolve *R*- and *S*-epimers in the HPLC operation consisted of 0.05 M ammonium acetate–methanol (50:3). The mobile phase employed to resolve the decarboxy-moxalactam consisted of a solution containing 5.2 g of tetra-*n*-butylammonium hydroxide (10% in water), 6.1 g of tetra-*n*-propylammonium hydroxide (10% in water), 1.0 g of dibasic sodium phosphate, and 1.0 g of monobasic sodium phosphate, adjusted to pH 6.0 by acetic acid, and methanol (7:3). The mobile phases were prepared by micropore filtration[7] and deaerated. No difference in absorbance between *R*- and *S*-epimers was observed at any wavelength of the UV spectrum (6). Accordingly, the peak areas of *R*- and *S*-epimers represent their intact concentrations. The calibration curves of the peak area against the concentration of moxalactam was satisfactorily linear.

Kinetic Procedure—All kinetic experiments were carried out at 37

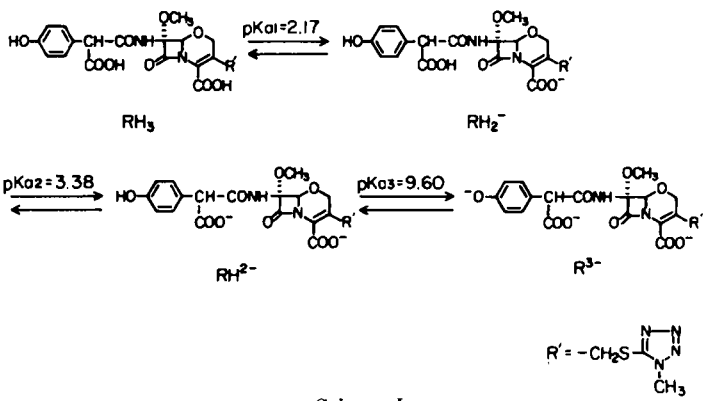

Scheme I

[1] Latamoxef; Shionogi & Co., Ltd., Osaka, Japan.

[2] pH-Stat titrator assembly consisting of TTT80 titrator, ABS80 autoburet, PHM84 research pH meter, REC80 servo graph, TTT81 digital titrator, and TIK801 titration keyboard; Radiometer, Copenhagen, Denmark.

[3] Radiometer PHM84 research pH meter.

[4] Waters ALC/GPC 204 series with U6K universal injector, Model 440 absorbance detector (254 nm), and Model M6000A pump, Waters Associates, Milford, Mass.

[5] Chromatopac C-E1B; Shimadzu, Kyoto, Japan.

[6] Nucleosil $7C_{18}$, particle size 5 μm; Macherey-Nagel Co., Düren, West Germany.

[7] 0.45 μm HAWP; Millipore Corp., Bedford, Mass.

0022-3549/84/0300-0369$01.00/0

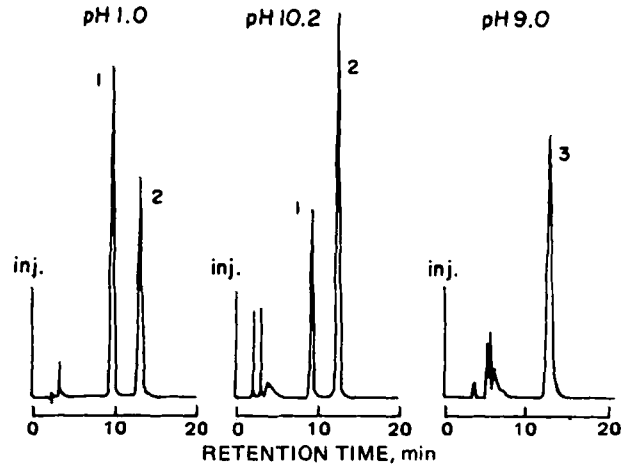

Figure 1—*Chromatograms at 254 nm for the reaction mixtures of moxalactam at pH 1.0 and 10.2 and the decarboxy-moxalactam at pH 9.0. Key: (1) R-epimer; (2) S-epimer; (3) decarboxy analogue.*

± 0.1°C and ionic strength 0.5 unless otherwise stated. The accurately weighed sample (*R*-epimer, *S*-epimer, or decarboxy-moxalactam) was dissolved in 1 mL of 0.5 M KCl and immediately diluted with 20 mL of 0.5 M KCl adjusted to the appropriate pH by the pH-stat and preheated to 37°C by a thermoregulator[8] with ±0.1°C precision. The final sample concentration was between 1×10^{-4} and 1×10^{-3} M. Portions were removed from the reaction solution at appropriate intervals and quickly frozen in a solid carbon dioxide–acetone bath. These were thawed just before HPLC analysis, and the remaining substances were determined.

Determination of Ionization Constants—The apparent ionization constants of moxalactam were determined potentiometrically (7) at ionic strength 0.5 and 37°C. The apparent ionization constants pK_{a1}, pK_{a2}, and pK_{a3}, which refer to the dissociation of the 4-carboxylic acid, the

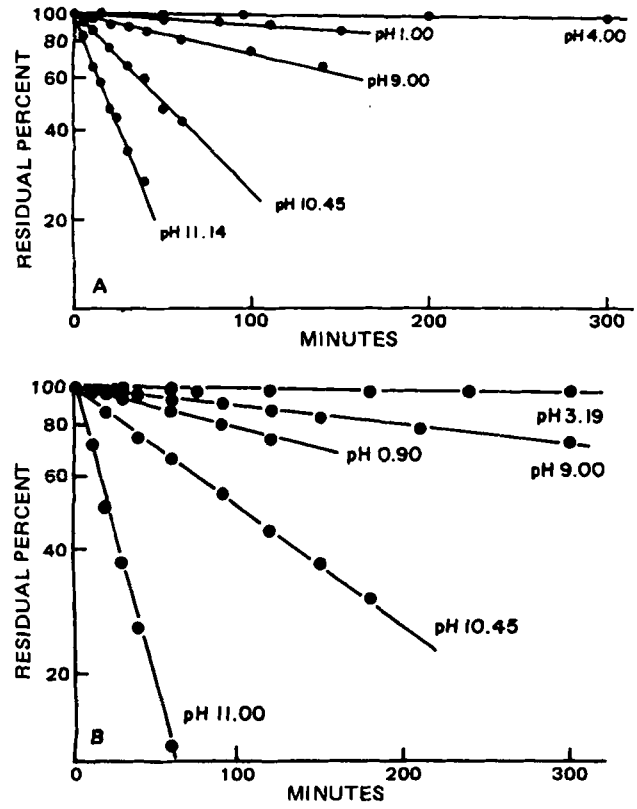

Figure 2—*Apparent first-order plots for moxalactam (A) and decarboxy-moxalactam (B) degradation at various pH values, 37°C, and ionic strength 0.5.*

[8] Taiyo Thermo Unit C-550; Taiyo Kagaku Kogyo Co., Ltd., Tokyo, Japan.

Table I—Rate Constants for Epimerization and Degradation of Moxalactam at 37°C and Ionic Strength 0.5

k_{pH}, h^{-1}	k_H, $M^{-1}h^{-1}$	k_a[a], h^{-1}	10^2k_b[a], h^{-1}	10^2k_c[b], h^{-1}	k_d[b], h^{-1}	k_{OH}, $M^{-1}h^{-1}$
k_1		2.37	0.61			3689
k_2		3.02	0.82			4127
k_3	0.477			0.42	0.584	210

[a] Rate constants defined in Eq. 6. [b] Rate constants defined in Eq. 7.

7-side chain carboxylic acid, and the phenol group, were 2.17, 3.38, and 9.60, respectively (Scheme I).

RESULTS AND DISCUSSION

Order of Degradation and Observed Rate Constants—Typical chromatograms of acidic (pH 1.0) and basic (pH 10.2) reaction mixtures, sampled at suitable times, are shown in Fig. 1, indicating that the *R*-epimer, the *S*-epimer, and the degradation products can be reasonably separated from one another. The chromatogram taken at pH 1.0 shows the reaction mixture which started with the *R*-epimer and that taken at pH 10.2 shows the reaction mixture which started with the *S*-epimer. Decarboxy-moxalactam, one of the degradation products, was found as a single broad peak with a longer retention time under the HPLC conditions which separated the *R*- and *S*-epimers. So, decarboxy-moxalactam is not shown in the chromatograms of the reaction mixtures starting with the *R*- and *S*-epimers in Fig. 1. Figure 1 also shows a typical chromatogram of the basic (pH 9.0) reaction mixture of the decarboxy-moxalactam. The parent compound can be separated from the degradation products.

As shown in Fig. 2, the semilogarithmic plots of the percent residual total moxalactam and the percent residual decarboxy-moxalactam *versus* time were reasonably linear and indicated that the degradation of the drug and its analogue followed pseudo-first-order kinetics at constant pH, temperature, and ionic strength 0.5 under various pH conditions. The disappearance of the *R*-epimer and the appearance of the *S*-epimer and *vice versa* were measured under various pH conditions. Figure 3 shows typical plots of the percent residual *R*- and *S*-epimers of the initial concentration of moxalactam, which is the total concentration of *R*- and *S*-epimers at the time when the first portion was removed, at pH 2.32, 2.36 and 10.20. A reversible epimerization was found to occur between *R*- and *S*-epimers. Furthermore, since the total amount of *R*- and *S*-epimers decreased in a semilogarithmic linear fashion with time as shown in Figs. 2A and 3, the *R*- and *S*-epimers probably decompose to other products with almost the same degradation rate constant. If either the *R*- or *S*-epimer decomposes faster than the other, the semilogarithmic plots of the percent residual moxalactam *versus* time must curve at the early stage of the decomposition.

From these results, the concentration–time profiles at various pH values are thought to be a consequence of the reaction illustrated in Scheme II, where k_1 is the epimerization rate constant from *R*-epimer to *S*-epimer, k_2 is the reverse, and k_3 is the degradation rate constant of moxalactam (*R*- and *S*-epimers).

According to Scheme II, the following kinetic equations can be written for the *R*- and *S*-epimers:

$$d(R)/dt = -k_1(R) + k_2(S) - k_3(R) \quad \text{(Eq. 1)}$$

$$d(S)/dt = k_1(R) - k_2(S) - k_3(S) \quad \text{(Eq. 2)}$$

The differential equations for *R*- and *S*-epimers (Eqs. 1 and 2) can be solved using Laplace transforms. The solutions of Eqs. 1 and 2 are:

$$(R) = \frac{(R_0)k_2 + (S_0)k_2}{k_1 + k_2} \cdot e^{-k_3 t} + \frac{(R_0)k_1 - (S_0)k_2}{k_1 + k_2} \cdot e^{-(k_1+k_2+k_3)t} \quad \text{(Eq. 3)}$$

$$(S) = \frac{(R_0)k_1 + (S_0)k_1}{k_1 + k_2} \cdot e^{-k_3 t} - \frac{(R_0)k_1 - (S_0)k_2}{k_1 + k_2} \cdot e^{-(k_1+k_2+k_3)t} \quad \text{(Eq. 4)}$$

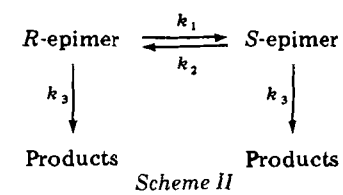

Scheme II

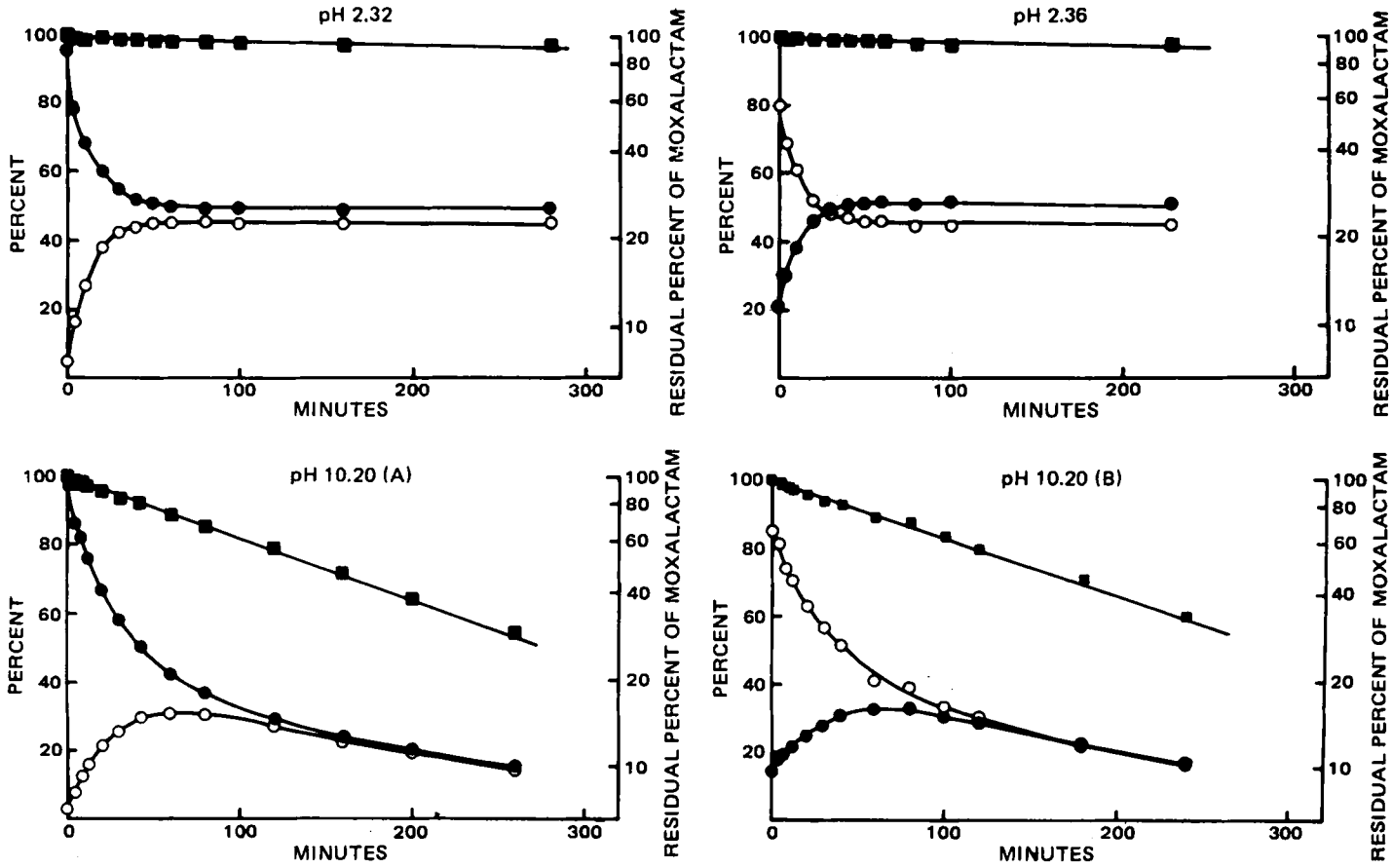

Figure 3—*Time courses for the* R-*epimer* (●), S-*epimer* (○), *and moxalactam (total of* R- *and* S-*epimers,* ■) *at pH 2.32 (disappearance of* R-*epimer and appearance of* S-*epimer), pH 2.36 (disappearance of* S-*epimer and appearance of* R-*epimer), and pH 10.2 [disappearance of* R-*epimer and appearance of* S-*epimer (A) and vice versa (B)], 37°C, and ionic strength 0.5. Moxalactam is semilogarithmically plotted* versus *time. The solid lines are the least-square fit (NONLIN) of the experimental data shown.*

$$(R) + (S) = [(R_0) + (S_0)]e^{-kst} \qquad \text{(Eq. 5)}$$

where (R) and (S) represent the concentrations of the R- and S-epimers at time t, and (R_0) and (S_0) represent the initial concentrations of R- and S-epimers, respectively. The experimental data, typified in Fig. 3, were fitted using the integrated forms of the equations through nonlinear regression analysis (NONLIN) (8) and yielded excellent fits to the theoretical solid lines calculated from Eqs. 3 and 4.

Primary Salt Effects—The primary salt effects on the epimerization of R- and S-epimers were studied at pH 3.50 and 37°C. The ionic strength was varied by adding potassium chloride. Figure 4 shows semilogarithmic plots of the apparent epimerization rate constant, k_{pH}, *versus* the square root of ionic strength ($\sqrt{\mu}$) based on an extended and modified form of the Debye–Hückel equation (9). Plots based on this equation should yield a linear relationship with a slope proportional to the product of the charges carried by the reactive species forming the activated complex. Although this modified equation holds, in theory, only up to an ionic strength of ~0.01, it has been shown to predict the kinetic salt effect reliably in some pharmaceutical systems to as high as an ionic strength of unity.

The slopes of the regression lines in Fig. 4 fitted to the data at pH 3.50 were slightly negative, −0.08 and −0.19 for k_1 and k_2, respectively. Neither of these slopes exactly fits any theoretical model predicted by the equation used, but their relatively low values are probably more consistent with the absence of ionic charge on at least one reactant rather than charges on all reactants.

Dissociation Equilibrium—In the pH range studied, moxalactam exists in four different forms: as free RH_3, a monoanion RH_2^-, a dianion RH^{2-}, and a trianion R^{3-}. Some reports indicate that the pK_a value of the carboxylic acid group at the 4-position of cephalosporins is between 1.9 and 2.9 (10, 11).

These results support the assignment of $pK_{a1} = 2.17$ to the carboxylic acid group at the 4-position of the drug. Accordingly, the value of $pK_{a2} = 3.38$ can be attributed to the carboxylic acid group in the 7-side chain. The apparent pK_a values of RH_3, RH_2^-, and RH^{2-} are 2.17, 3.38, and 9.60, respectively (Scheme I).

pH–Rate Profile—The pH dependencies of overall first-order rate constants k_1 and k_2 of moxalactam epimerization and k_3 of moxalactam degradation at 37°C and ionic strength 0.5, are shown in Figs. 5 and 6. Figure 5 shows that the observed rates of the epimerization increased rapidly and uniformly with increasing pH above pH 7.5. Since the slopes of these straight-line portions of log k_{pH} *versus* pH profiles are unity, it is likely that dissociation of the phenolic group has no effect on the epimerization, and the specific hydroxide ion-catalyzed reactions of RH^{2-} and R^{3-} take place at almost the same rate in this pH region.

The profiles bent over to constant rates at pH values lower than pH 4, indicating that a dissociation constant, pK_{a2}, affected the epimerization rates. But the two reaction mechanisms, the hydrogen ion-catalyzed epimerization reaction of RH^{2-} and the water-catalyzed epimerization

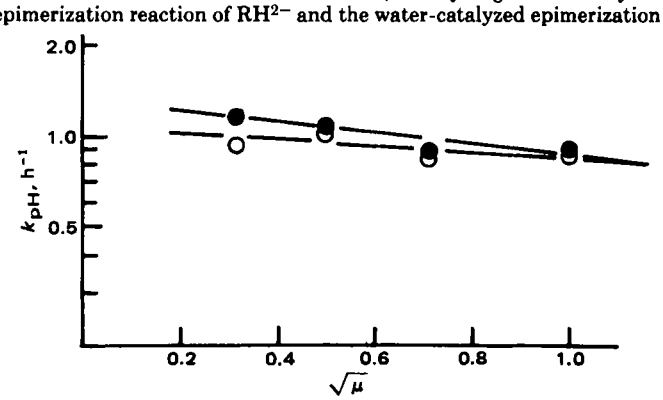

Figure 4—*Semilogarithmic plots of* k_{pH} versus *the square root of ionic strength* ($\sqrt{\mu}$) *for the epimerization of moxalactam at pH 3.50 and 37°C. Key:* (○) k_1; (●) k_2.

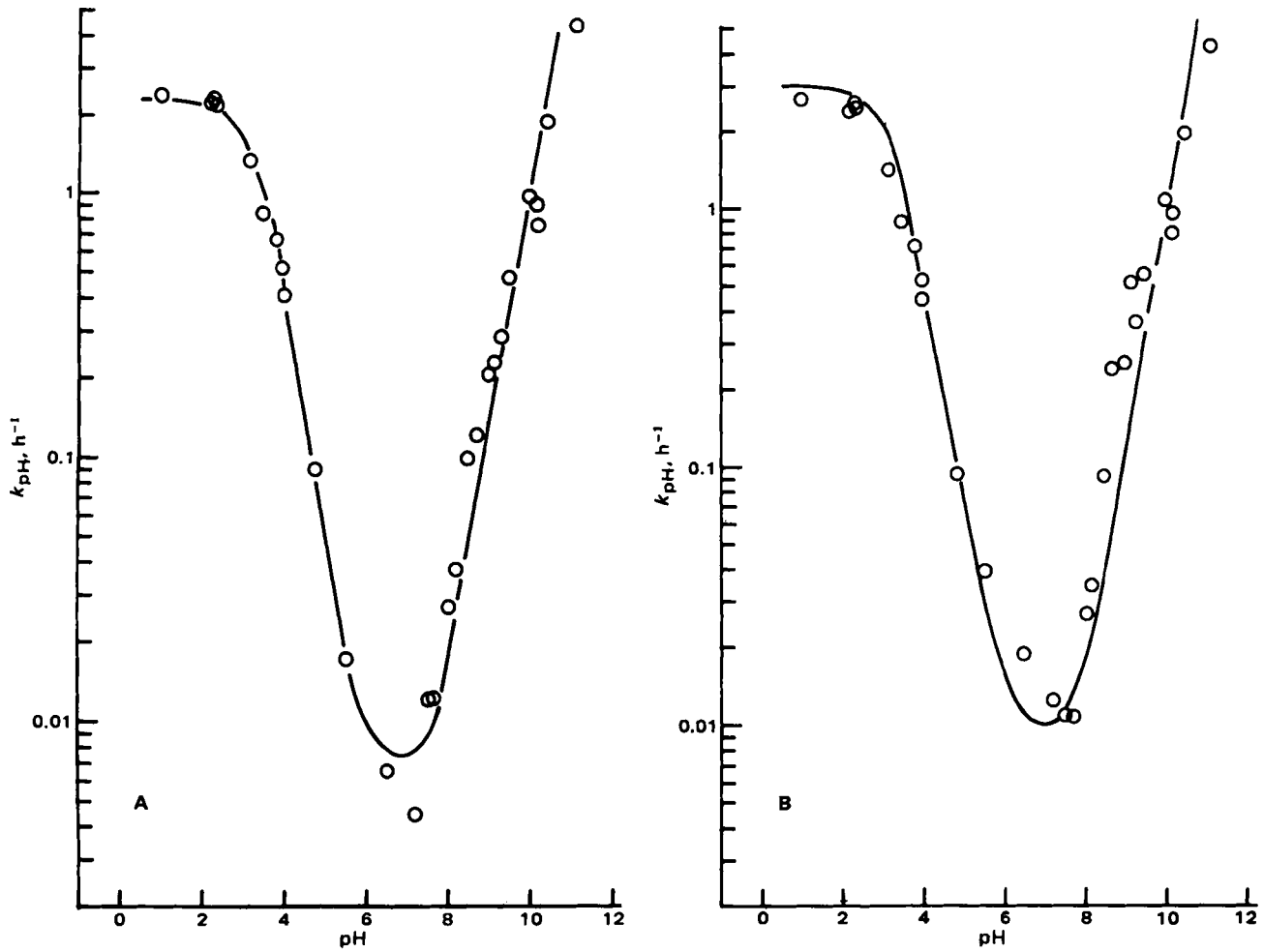

Figure 5—*Log k_{pH}–pH profile for moxalactam epimerization in aqueous solution at 37°C and ionic strength 0.5. The points are experimental values and the solid line is the theoretical curve calculated from Eq. 6 and the constants in Table I. Key: (A) k_1; (B) k_2.*

reactions of RH_3 and RH_2^- (undissociated moxalactam of the 7-side chain carboxylic acid group), give the same pH–rate profile and are kinetically equivalent in this pH range. However, it is possible to distinguish between the two reaction mechanisms according to the results of the primary salt effect of *R*- and *S*-epimers. The near lack of the primary salt effect at pH 3.50, where the concentrations of the undissociated and dissociated forms of the 7-side chain carboxylic acid group are almost the same (Fig. 4) indicates that the water-catalyzed epimerization reactions may occur below pH 6. Proton abstraction, which is important for epimerization, by the water-catalyzed reaction is more likely to occur than the hydrogen ion-catalyzed reaction due to water having stronger basicity than the hydrogen ion.

The total shape of log *k versus* pH profiles of moxalactam epimerization (k_1 and k_2) can be expressed by the following rate law:

$$k_{pH} = k_a\left(\frac{a_H}{K_{a2} + a_H}\right) + k_b + k_{OH}\left(\frac{K_w}{a_H}\right) \qquad \text{(Eq. 6)}$$

where k_a and k_b are the first-order rate constants of the undissociated and dissociated forms of the 7-side chain carboxylic acid group for the water-catalyzed epimerization, respectively, k_{OH} is the second-order rate constant for the hydroxide ion-catalyzed epimerization, and a_H and K_{a2} are the activity of hydrogen ion measured by the glass electrode and the dissociation constant of the 7-side chain carboxylic acid group, respectively. The value for the autoprotolysis constant of water, K_w, at 37°C is 2.38×10^{-14} (12). The solid lines in Fig. 5 represent the theoretical curves calculated by NONLIN and the points are the experimental results. The rate constants k_1 and k_2 with the best fits of the observed rate–pH profiles are given in Table I.

Figure 6 shows the log k_{pH}–pH profile for the degradation of moxalactam (k_3). The observed rate of the degradation decreased uniformly with increasing pH, and the slope of the straight-line portion of the log k_{pH} *versus* pH curve is negative unity below pH 2.5. The degradation rate of moxalactam between pH 4 and 6 showed pH independence, although there was a little dispersion. This implies that the overall degradation consists of the water-catalyzed or spontaneous reactions of moxalactam. Such a pH-independent degradation is known to be a common feature for the degradation of the β-lactam moiety of cephalosporins (10). There was a sigmoid dependence of k_{pH} on pH at pH values near pK_{a3}, followed by a rapid decrease of almost positive unity as the pH decreased. This inflection indicates that the degradation rate was influenced by the dissociation equilibria of the 7-side chain phenolic group (pK_{a3}). The observed rate of the degradation increased by positive unity with increasing pH above pH 10.5, which shows the hydroxide ion-catalyzed degradation.

The total shape of the log k_{pH}–pH profile of moxalactam degradation can be expressed by the following rate law:

$$k_{pH} = k_H a_H + k_c + k_d\left(\frac{K_{a3}}{K_{a3} + a_H}\right) + k_{OH}\left(\frac{K_w}{a_H}\right) \qquad \text{(Eq. 7)}$$

where k_c and k_d represent the first-order rate constants for the water-catalyzed degradation of dianionic and trianionic moxalactam, k_H and k_{OH} represent the second-order rate constants for the specific hydrogen ion-catalyzed and specific hydroxide ion-catalyzed degradation, and K_{a3} is the dissociation constant of the 7-side chain phenolic group.

In Fig. 6, the solid line represents the theoretical curve calculated by NONLIN. The rate constants in Eq. 7 that produced the best fit to the observed rate–pH profile are given in Table I; the white circles show the experimental results. The good agreement indicates that this equation adequately describes the kinetics of moxalactam degradation. The solid circles in Fig. 6 show the degradation rates of the decarboxy-moxalactam obtained from the slopes in Fig. 2B. The degradation rate of the drug is 1.5–3 times as large as the degradation rate of the decarboxy-moxalactam at pH 7.5 and 9.0, and little difference exists between the degradation rates at pH 0.9, 3.1, 10.2, and 11.0. These results suggest that a sigmoidal dependency of the degradation rate on pH below pH 10 comes from the spontaneous decarboxylation reaction of the dissociated moxalactam of

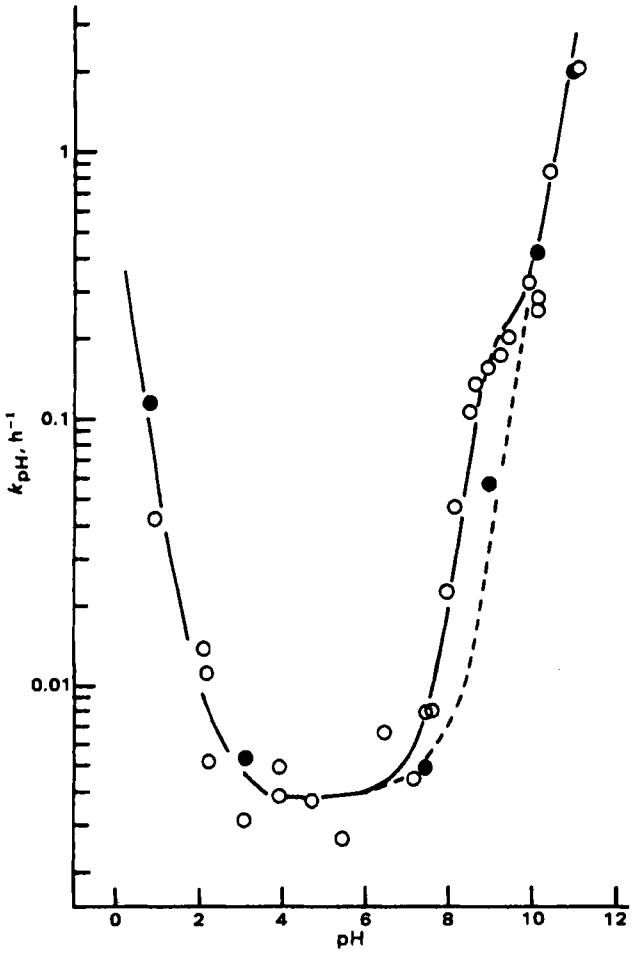

Figure 6—*Log k_{pH}–pH profiles for moxalactam (○) degradation (k_3) and the decarboxy-moxalactam (●) in aqueous solution at 37°C and ionic strength 0.5. The points are experimental values, and the solid line is the theoretical curve of moxalactam calculated from Eq. 7 and the constants in Table I.*

the 7-side chain phenolic group in parallel with the specific hydroxide ion-catalyzed degradation of the drug.

Epimerization Mechanism—The pH–epimerization rate profiles yielded straight lines with a slope of unity verifying first-order dependence on hydroxide ion in the basic region. The mechanism for the epimerization reaction can be written in terms of the abstraction of the α-proton by hydroxide ion leading to the formation of a planar carbanion (2). The mechanism for the epimerization reaction in the acidic region can be explained by the abstraction of the α-proton by water mainly from the undissociated moxalactam of the 7-side chain carboxylic acid group to the formation of a planar carbanion.

The relative order of k_a and k_b in Table I agrees with the decrease in electron-withdrawing by the dissociation of the 7-side chain carboxylic acid group attached to the α-carbon and causes a corresponding decrease in the rate of epimerization. On the other hand, the dissociation of the 7-side chain phenolic group had little influence on the epimerization rates. This is because the contribution of hydroxide ion toward the α-proton abstraction dominates in the basic region, and the influence of the dissociation of the phenolic group may disappear. However, factors other than the inductive effect of the substituents attached to the α-carbon may be considered in determining the rate of epimerization, as the stability of an enolate intermediate consisting of an amido or a carboxylic acid group resulting from the α-proton abstraction.

REFERENCES

(1) R. Wise, P. J. Wills, and K. A. Bedford, *Antimicrob. Agents Chemother.*, **20**, 30 (1981).

(2) A. Tsuji, Y. Itatani, and T. Yamana, *J. Pharm. Sci.*, **66**, 1004 (1977).

(3) H. Bundgaard, *Int. J. Pharm.*, **5**, 257 (1980).

(4) M. Narisada, T. Yoshida, H. Onoue, M. Ohtani, T. Okada, T. Tsuji, I. Kikkawa, N. Haga, H. Satoh, H. Itani, and W. Nagata, *J. Med. Chem.*, **22**, 757 (1979).

(5) T. Yoshida, S. Matsuura, M. Mayama, Y. Kameda, and S. Kuwahara, *Antimicrob. Agents Chemother.*, **17**, 302 (1980).

(6) R. Konaka, K. Kuruma, R. Nishimura, Y. Kimura, and T. Yoshida, *J. Chromatogr.*, **225**, 169 (1981).

(7) A. Albert and E. P. Serjeant, "The Determination of Ionization Constants," Chapman and Hall, London, England, 1971, chaps. 2 and 3.

(8) C. M. Metzler, "NONLIN, A Computer Program for Parameter Estimation in Nonlinear Situations," The Upjohn Co., Kalamazoo, Mich., 1969.

(9) A. N. Martin, J. Swarbrick, and A. Cammarata, "Physical Pharmacy," Lea & Febiger, Philadelphia, Pa., 1969, pp. 380, 381.

(10) T. Yamana and A. Tsuji, *J. Pharm. Sci.*, **65**, 1563 (1976).

(11) E. C. Rickard and G. C. Cooke, *J. Pharm. Sci.*, **66**, 379 (1977).

(12) H. S. Harned and W. J. Hamer, *J. Am. Chem. Soc.*, **55**, 2194 (1933).

ACKNOWLEDGMENTS

The authors thank Professor Akira Tsuji, Faculty of Pharmaceutical Science of Kanazawa University, for his generous support and timely advice and Drs. Kaoru Kuriyama and Hiroshi Tanida for their helpful discussions.